



Stabilization and electro-optical switching of liquid crystal blue phases using unpolymerized and polymerized polyoxometalate-based nanoparticles

Jiao Wang, Chang-Gen Lin, Juntao Li, Jie Wei, Yu-Fei Song & Jinbao Guo

To cite this article: Jiao Wang, Chang-Gen Lin, Juntao Li, Jie Wei, Yu-Fei Song & Jinbao Guo (2016) Stabilization and electro-optical switching of liquid crystal blue phases using unpolymerized and polymerized polyoxometalate-based nanoparticles, *Molecular Crystals and Liquid Crystals*, 634:1, 12-23, DOI: [10.1080/15421406.2016.1177900](https://doi.org/10.1080/15421406.2016.1177900)

To link to this article: <http://dx.doi.org/10.1080/15421406.2016.1177900>



Published online: 26 Sep 2016.



Submit your article to this journal [↗](#)



Article views: 47



View related articles [↗](#)



View Crossmark data [↗](#)

Stabilization and electro-optical switching of liquid crystal blue phases using unpolymerized and polymerized polyoxometalate-based nanoparticles

Jiao Wang^a, Chang-Gen Lin^b, Juntao Li^a, Jie Wei^a, Yu-Fei Song^b, and Jinbao Guo^a

^aCollege of Materials Science and Engineering, Beijing University of Chemical Technology, Beijing, P. R China;

^bState Key Laboratory of Chemical Resource Engineering, Beijing University of Chemical Technology, Beijing, P. R. China

ABSTRACT





In this study, unpolymerizable and polymerizable polyoxometalate (POM)-based nanoparticles have been developed for the stabilization of liquid crystal blue phase (LC-BPs). The result demonstrates that BPs could be stabilized with the help of doped unpolymerizable POM nanoparticles, leading to widening of the temperature range of BP. Meanwhile, photo polymerization of polymerizable POM-based nanoparticle allows for the formation of POM-based polymer networks into the disclination lines in polymer stabilized BPs, yielding the stabilization of BPs. Remarkably, the participation of the polymer network formation of POM-based nanoparticle could be visualized by energy-dispersive X-ray elemental maps due to the existence of tungsten. Finally, electro-optical switching of polymer stabilized BPs based on the Kerr effect has been investigated in detail. POM-based polymer networks within disclination lines yield a decrease in free energy of BP system, thus enabling a reduction in the switching voltage of the BP device. These results are significant contributions to the BP fundamental research and the technical progress in areas of LC photonic application.

KEYWORDS

Polyoxometalate-based nanoparticles; liquid crystal blue phases; polymer network; stabilization; electro-optical switching

1. Introduction

Nanoparticle-doped liquid crystals (LCs) are attracting growing interest due to the novel properties that emerge in these nano-systems. To date, various nanomaterials, from metal nanoparticles to quantum dots have been introduced into LCs, and various effects on the properties of LCs have been investigated [1,2]. Among the various LC phases, blue phases (BPs) with three-dimensional (3 D) superstructures have gained much attention in recent years due to their applications in many fields, such as LC displays, tunable LC laser and optical sensors [3–11]. BPs could be classified into three types: BP_{III}, BP_{II}, and BP_I on the cooling process with amorphous symmetric, simple cubic, and body centered cubic structures, respectively [3]. Since the BP-based LCD panels were demonstrated by Samsung electronics, the investigations of BPs for LCD applications have gained increasing attention due to their

CONTACT Jinbao Guo  guojb@mail.buct.edu.cn  College of Materials Science and Engineering, Beijing University of Chemical Technology, Beijing 100029, P.R. China; Yu-Fei Song  songyf@mail.buct.edu.cn  State Key Laboratory of Chemical Resource Engineering, Beijing University of Chemical Technology, Beijing 100029, P.R. China.

Jiao Wang, Chang-Gen Lin and Juntao Li contributed equally to this work.

Color versions of one or more of the figures in the article can be found online at www.tandfonline.com/gmcl.

fast switching times, insensitivity to the cell gap, and alignment layer-free nature. Considering the practical application to display technologies, BPs still have some problems, such as narrow temperature ranges, high operating voltage, hysteresis, and residual transmittance. In order to address these issues, much effort has been paid to extend the BP ranges and optimize the electro-optical performance during these years, including polymer network, nanoparticles and various molecule structures such as T-shaped molecules, dimer molecules and bent-core molecules[12–26].

Among them, nanoparticles trapped in the disclination lines have been shown to stabilize the BP by removing the effective volume of the high energy-costing disclination lines. Until now, various nanomaterials, such as CdSe nanoparticle, gold nanoparticle have been introduced into LCs to induce BP with a wide temperature range [23–26]. For example, H. Yoshida *et al.*, report the expansion of the temperature range of BPs by doping spherical gold nanoparticles with a mean diameter of 3.7 nm in LC mixture. They found that the temperature range of the BPs was increased from 0.5 to 5°C [22]. H. Yang *et al.*, demonstrated that BPI could be stabilized by a small amount of hydrophobic surface-treated ZnS nanoparticles with an average diameter of around 33 nm, in which the temperature range of BPI was extended even up to about 15.6°C. In addition, the reversible electro-optical switching was achieved which could be considered as hysteresis-free at a 0.5–0.7 wt% doping level. They thought that the above phenomena rise from the fact that the volume and the free energy around the disclinations were suppressed by introducing the nanoparticles [25].

Polyoxometalates (POMs), representing a diverse range of nanosized clusters of V, Mo, W, Nb, and so on, have evoked a lot of interests due to their precise chemical structures, rich topologies, uniform size and interesting physical properties [27–32]. Among them, the development of organic-inorganic hybrid POMs has attracted much attention because they hold considerable potential for functional materials [31–32]. In this study, we develop unpolymerizable and ultraviolet (UV)-polymerizable POM-based nanoparticles to stabilize BPs. Here the polymerizable POM-based nanoparticle has been fabricated by grafting two polymerizable acrylate groups onto POM precursor, and then sequentially polymerized to form polymer network by integrating diacrylate LC monomers in LC mixture. We firstly investigate the effects of unpolymerizable POM nanoparticle (d-1.0 nm) and polymer networks from polymerizable POM-based nanoparticle on extending the temperature range of BPs. Then the corresponding mechanisms stabilizing the BPs have been discussed in detail. Finally, we study the electro-optical performances based on the Kerr effect for the POM-based polymer stabilized BPs. This work opens up a new way for developing the BP system that exhibit wide temperature range and good electric-optical switching effect, thereby leading to the potential applications in areas of display as well as optoelectronic devices.

2. Experimental sections

2.1. Materials

Nematic LCs, BYLC-X ($\Delta n = 0.20$ at 589 nm wavelength and 20°C; Beijing Bayi Space LCD Technology CO., LTD.); S811 (chiral dopant, Beijing Lyra Tech); Diacrylate photo-polymerizable LCs monomer, C6M and photoinitiator, 2, 2-dimethoxy-2-phenylacetophenone (Irgacure 651, TCI Co. Ltd.) were used. Diacrylatenematic monomer, C6M was synthesized according to the method suggested by D. J. Broer *et al.* [33]. $[(C_4H_9)_4N]_4[(SiW_{11}O_{39})O\{Si(CH_2)_3NH_2 \cdot HCl\}_2]$ (POM precursor, $SiW_{11}-NH_2$), was

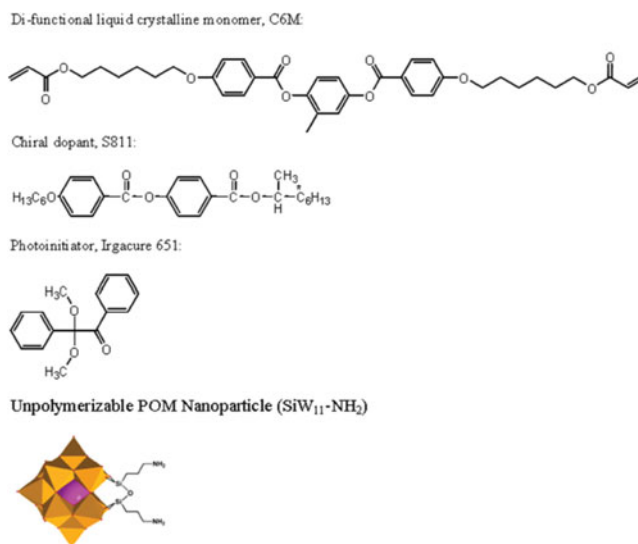


Figure 1. The chemical structures of C6M, S811, Irgacure 651 and $\text{SiW}_{11}\text{-NH}_2$.

prepared according to the published procedure and fully characterized [34]. Fig. 1 shows the chemical structures of C6M, S811, Irgacure 651 and POM precursor, $\text{SiW}_{11}\text{-NH}_2$.

2.2. Synthesis of polymerizable POM nanoparticle

$[(\text{C}_4\text{H}_9)_4\text{N}]_4[(\text{SiW}_{11}\text{O}_{39})_3\text{O}\{\text{Si}(\text{CH}_2)_3\text{NHCO}(\text{CH}_2)_2\text{OOCCHCH}_2\}_2]$ was directly prepared according to our previous work [31]. Yield: 56.9%.

$^1\text{H-NMR}$ ($\text{CD}_3\text{CN-}d_3$, ppm): $\delta = 0.72$ (t, 4 H), 0.99 (t, 48 H), 1.40 (m, 32 H), 1.62 (m, 32 H), 1.75 (m, 4 H), 2.49 (m, 4 H), 3.15 (t, 32 H), 3.26 (m, 4 H), 4.32 (m, 4 H), 5.92 (t, 2 H), 6.16 (m, 2 H), 6.37 (d, 2 H).

$^{13}\text{C-NMR}$ ($\text{DMSO-}d_6$, ppm): $\delta = 8.67, 13.48, 19.19, 23.05, 34.52, 41.38, 45.85, 57.52, 128.22, 131.58, 163.16, 168.85$.

$^{29}\text{Si-NMR}$ ($\text{DMSO-}d_6$, ppm): $\delta = -52.95, -85.27$.

FT-IR (KBr, cm^{-1}): $\nu = 3390, 2962, 2932, 2873, 1725, 1662, 1541, 1482, 1382, 1273, 1187, 1113, 1044, 967, 920, 855, 805, 619, 533, 420$.

Elemental analysis (%) calcd. for $\text{C}_{82}\text{H}_{172}\text{N}_6\text{O}_{46}\text{Si}_3\text{W}_{11}$ (4084.75): C 24.09, H 4.21, N 2.06; found: C 23.83, H 4.14, N 1.96.

2.3. Preparation of BPs sample and polymer stabilized BPs

Cells with indium tin oxide (ITO) electrode were made from two pieces of glass bonded together, where PE film of 12 μm thickness was used as the cell spacers and no surface alignment layer was used. The samples were filled into the cells by capillary action at appropriate temperature. For the conventional LC cells, a homogeneous mixture of BYLC-X, S811 and unpolymerizable POM nanoparticle with appropriate weigh ratio was filled into glass cell, and the compositions of the sample are listed in Table 1. For the polymer stabilized BPs, the LC mixtures containing BYLC-X, S811, polymerizable POM nanoparticle, C6M, and Irgacure 651 were filled into the cell at an isotropic state and cooled down to BP temperature at a rate of $0.5^\circ\text{C}/\text{min}$, then subsequently the cell was irradiated upon 365 nm UV light ($1.5 \text{ mW}/\text{cm}^2$)

Table 1. Compositions and transition temperatures of LC samples ^a ΔT : BP temperature range.

Sample no.	Composition/wt%				Transition temperature/ $^{\circ}\text{C}$		
	POM nanoparticles		S811	BYLC-X	N*-BP	BP-I	ΔT^a
A0	None	0	33	67	53.3	47.4	5.9
A1	SiW ₁₁ -NH ₂	0.1	33	67	52.6	42.5	10.1
A2	SiW ₁₁ -NH ₂	0.5	33	67	52.9	42.6	10.3
A3	SiW ₁₁ -NH ₂	0.8	33	67	51.8	42.2	9.6
A4	SiW ₁₁ -NH ₂	1	33	67	47.8	30.4	17.4
A5	SiW ₁₁ -NH ₂	1.2	33	67	48.5	35.3	13.2
A6	SiW ₁₁ -NH ₂	1.5	33	67	51.8	44.1	7.7
B1	SiW ₁₁ -NH ₂ aggregates	0.1	33	67	49.4	39.9	9.5
B2	SiW ₁₁ -NH ₂ aggregates	0.5	33	67	52.4	41.5	10.9
B3	SiW ₁₁ -NH ₂ aggregates	0.8	33	67	51.4	42.5	8.9
B4	SiW ₁₁ -NH ₂ aggregates	1	33	67	52.1	40.4	11.7
B5	SiW ₁₁ -NH ₂ aggregates	1.2	33	67	54.6	45.2	9.4
B6	SiW ₁₁ -NH ₂ aggregates	1.5	33	67	51.8	43	8.8

for 15 min in a temperature range where a BPI phase forms. In this fabrication process, the temperature of the LC cell was carefully changed so as to keep BPI phase during UV exposure.

2.4. Characterization of polymerizable POM nanoparticle

¹H-NMR, ¹³C-NMR, and ²⁹Si-NMR spectra were obtained on a Bruker AV400 NMR spectrometer at resonance frequency of 400 MHz. Fourier transform infrared (FT-IR) spectra were carried out on a Bruker Vector 22 infrared spectrometer using KBr pellet method. Electrospray ionization mass spectra (ESI-MS) were recorded on a Xevo G2 QT ESI-MS calibrated using a 5 mM sodium formate solution in 90:10 2-propanol:water, and all experiments were performed in negative mode using acetonitrile as solvent. Elemental Analyses were completed by using varioEL cube from Elementar Analysensysteme GmbH. Transmission electron microscopy (TEM) micrographs were performed using a Tecnai G2 20 instrument.

2.5. Measurement and characterization of LC samples

The samples were observed using a polarizing light microscope (POM) (Leica, DM2500P) with a heating stage of an accuracy of $\pm 0.1^{\circ}\text{C}$ (LTS 420). The optical images were recorded using Linksys 2.43 software. The reflection spectra were obtained by fiber spectrometer (Avantes, AvaSpec-2048). The surface morphology and cross-section of the polymer network was observed by scanning electron microscopy (SEM) (Hitachi S-4700). Optical transmittance was measured for a LC sample in the in-plane-switching (IPS) cells under the crossed polarizers (Instrument System, DMS505-101), as a function of applied square wave voltage of 1 kHz. The samples in IPS cells were placed at an inclination angle θ of 45° with respect to incident light, and the temperature was controlled with a hot stage calibrated to an accuracy of $\pm 0.1^{\circ}\text{C}$ (LTS 420). The IPS cells were purchased from Bayi Space LCD Technology Corporation, and the indium tin oxide electrode width was $12.0\ \mu\text{m}$, the distance between the electrodes was $15.0\ \mu\text{m}$, and the cell gap was maintained at $3.8\ \mu\text{m}$ by spacers.

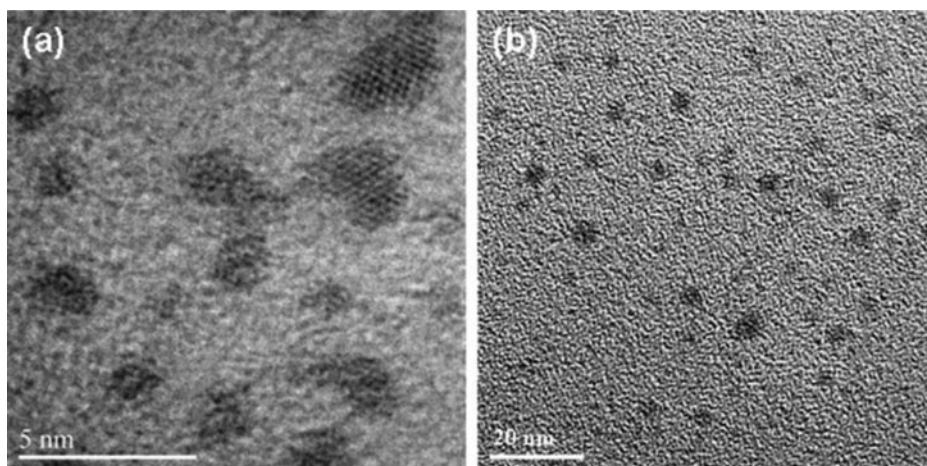


Figure 2. TEM images of (a): monodispersed SiW₁₁-NH₂ nanoparticle and (b): the corresponding aggregates.

3. Results and discussion

3.1. Temperature range of BPs induced by unpolymerizable POMs nanoparticles

We firstly investigate the effect of unpolymerizable POMs nanoparticle (POM precursor and its aggregate) on the stabilization of BPs. Here POM precursor, SiW₁₁-NH₂ (Fig. 1) was encapsulated with tetrabutyl ammonium using a method described in previous study [34]. As a demonstration of TEM image in Fig. 2a, the monodispersed POM precursor has an average diameter of 1–1.5 nm. Then we prepared a series of LC samples A1-A6 as listed in Table 1, in which the weigh ratio of POM precursor SiW₁₁-NH₂ ranges from 0 wt% to 1.5 wt%. The LC samples are placed in a heat stage, heated into the isotropic phase and then slowly cooled at 0.5°C/min. As listed in Table 1 and Fig. 3a, it clearly indicates that SiW₁₁-NH₂ nanoparticle could serve to stabilize BPs by comparing the doped samples A1-A6 with undoped sample A0. Meanwhile, the clearing points of all the samples decrease which attributes to the introduction of POM precursor SiW₁₁-NH₂. By increasing SiW₁₁-NH₂ content from 0 to 1.0 wt%, the BP temperature ranges increase from 5.9°C to 17.4°C in samples A0-A4. As a typical sample, the phase sequence of the sample A4 on cooling process is from the isotropic phase (I), BP I to Ch with a BP temperature range of $\Delta T \approx 17.4^\circ\text{C}$. However, further increasing of the concentration of the SiW₁₁-NH₂ nanoparticle from 1.2 wt% to 1.5 wt% in A5 and A6 suppresses the BP range as shown in Fig. 3a, which we think may be due to the concentration effect of POM hybrid precursor in LC system as indicated in previous study [25].

Additionally, we provide the polarized light microscope images for the doped BP sample with 1.0 wt% POM precursor (A4) in Fig. 3b. In this sample, colored platelets started to nucleate at a certain temperature, and they gradually grew in number and size to fill the whole field of view. What's more, we find that there is no obvious phase transition in these LC samples. To understand precisely the phase behavior upon cooling, the temperature dependence of the Bragg reflection of sample A4 was provided as a typical sample. Fig. 3c illustrates the Bragg reflection wavelength of the doped sample (A4) as a function temperature. It clearly shows a continuous change in the temperature dependence of the Bragg reflection wavelength, which

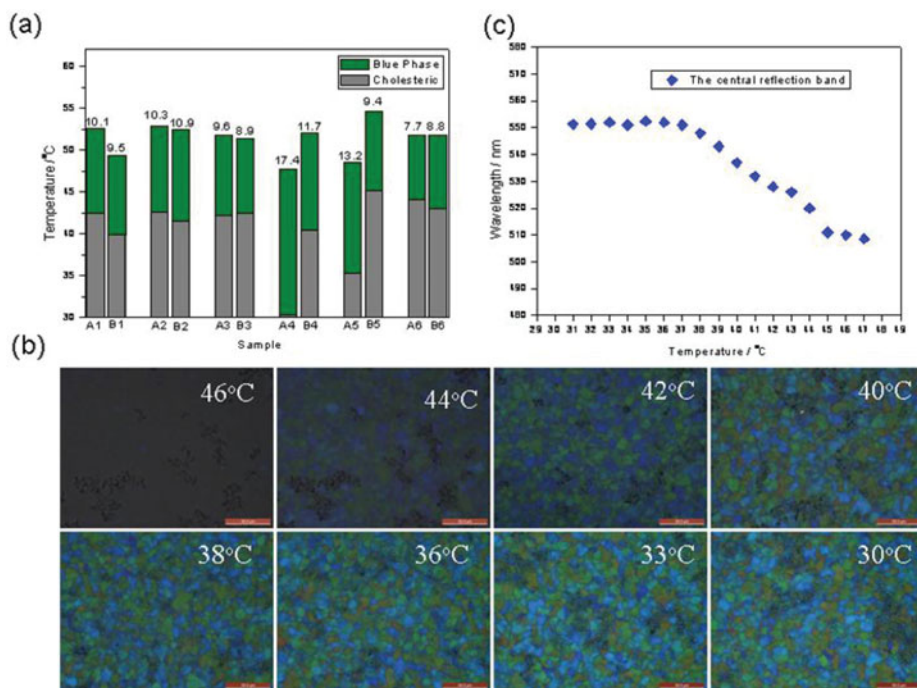


Figure 3. (a): BP temperature ranges of samples A1–A6 and B1–B6. The temperature range of BP (green area) is marked on the columns in the chart; (b): Polarized light microscope images of BP textures of sample A4 at different temperatures and (c): The reflection band of sample A4 as a function of temperature.

reveals that no phase transition from BPII and BPI happened as demonstrated in the previous study [6]. Based on the polarized light microscope and Bragg reflection observations, it is apparent that the doped LC samples in this study possess no BPII during the cooling process.

In order to evaluate the size of POM nanoparticle on the thermodynamic BPs, we note that $\text{SiW}_{11}\text{-NH}_2$ could spontaneously aggregate into reverse micelles with a larger size in a mixed solvent, wherein the hydrophilic head of POM is inside and the hydrophobic alkyl chain is outside [31]. TEM image in Fig. 2b confirms the nanospherical morphology of the $\text{SiW}_{11}\text{-NH}_2$ aggregates with a diameter of around 5 nm. By comparing the BP temperature ranges of the LC samples B1–B6 (doped with $\text{SiW}_{11}\text{-NH}_2$ aggregates) with A1–A6 ($\text{SiW}_{11}\text{-NH}_2$), we find that POM aggregates have similar stabilization effect for BPs as shown in Table 1 and Fig. 3a. In fact, $\text{SiW}_{11}\text{-NH}_2$ nanoparticle might be inclined to aggregate to form large-size aggregates in LC media due to their structural characteristics and surface functional groups. These observations may be explained due to the fact that is similar to other nanoparticles [23–26], $\text{SiW}_{11}\text{-NH}_2$ nanoparticles and their aggregates doped in BPs may be trapped in the disclination lines due to the elastic interactions. As a result, the free energy associated with the energetically costly disclination region has been reduced. A possible schematic for the POM nanoparticle-stabilized BP I is illustrated in Fig. 4, here the disclination cores between the double-twisted cylinders (DTC) were filled with $\text{SiW}_{11}\text{-NH}_2$ nanoparticle or the corresponding aggregates, thereby leading to the stabilization of the disclination lattice of BPI. Increasing the concentration of POM nanoparticle yields a continuously suppression of the volume and the free energy around the disclinations. However, if the concentration was too high, the BPI would be disturbed as mentioned above. To sum up, the stabilizing mechanism of the BP for both $\text{SiW}_{11}\text{-NH}_2$ nanoparticle and the corresponding aggregates may be attributed to a decrease in the free energy caused by self-organization-assisted nanoparticles assembly [26].

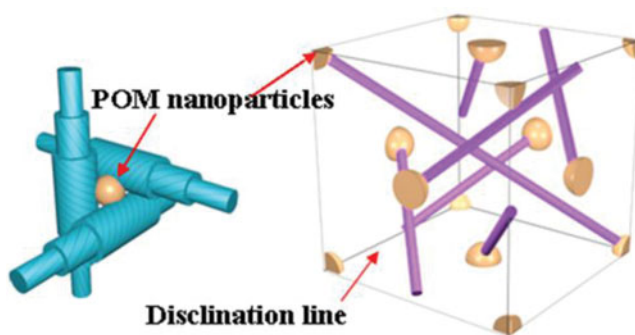


Figure 4. The disclination core between the double-twisted cylinders filled with POM nanoparticles and the corresponding disclination lattices of BPI.

3.2. Stabilization of BPs using polymer network based on polymerizable POM nanoparticle

As known that, in addition to the nanoparticles, the polymer stabilized BPs is another effective way to stabilize BPs [4]. To demonstrate this polymer stabilized effect as well as directly observe the POM moiety existence in BP system, we prepared a polymerizable POM-based nanoparticle containing two acrylate groups based on the above POM precursor as shown in Fig. 5a. The structural conformation of polymerized POM-based monomer was confirmed by different techniques. In the FT-IR spectrum, typical amide C = O stretching vibration bond could be observed at *ca.* 1625 cm^{-1} , and characteristic $\text{SiW}_{11}\text{-NH}_2$ stretching vibrations can be found at *ca.* 1044 (Si-O-Si), 967 ($\text{W}=\text{O}$), and 855 (W-O-W) cm^{-1} , suggesting organic moieties have been successfully grafted onto POM clusters. $^1\text{H-NMR}$ spectrum of polymerized POM-based monomer shows signals that can be unambiguously assigned and fits well with the corresponding molecular structure. In the $^{29}\text{Si-NMR}$ spectra,

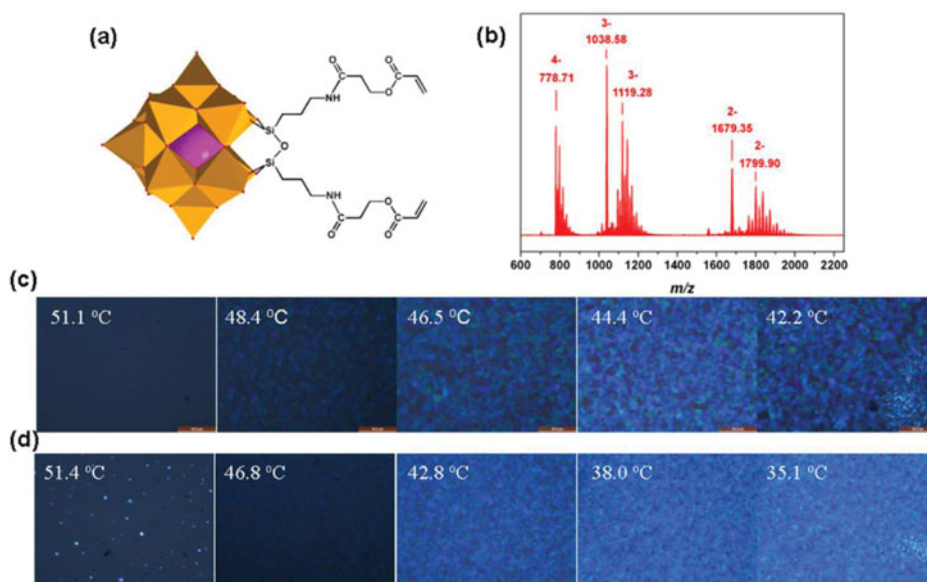


Figure 5. (a): The chemical structure of polymerized POM-based monomer; (b): the corresponding ESI-MS spectra; (c): Polarized light microscope images of sample C1 before polymerization and (d): after polymerization.

Table 2. The compositions of samples C1 and C2 and the corresponding phase temperatures of them before and after polymerization.

Sample no.	Composition/wt% ^a				Transition temperature/°C					
	POM Monomer	C6M	S811	BYLC-X	Before polymerization			After polymerization		
					N*-BP	BP-I	ΔT ^b	N*-BP	BP-I	ΔT
C1	1.0	0.5	33.0	66.5	51.7	42.2	8.9	51.5	35.2	16.3
C2	1.0	1.0	33.0	66.0	51.9	44.2	7.7	51.4	38.3	13.1

^a2% by weight of monomers of photo initiator Irgacure 651 is added.^bΔT: BP temperature range.

peaks observed at *ca.* −53 and −85 ppm correspond to the Si in silane and the Si of the monolacunary SiW₁₁ cluster, respectively. The molecular structure of polymerized POM-based monomer was further investigated by ESI-MS as shown in Fig. 5b. Peaks at *m/z* 778.71 can be ascribed to [(SiW₁₁O₃₉)O{Si(CH₂)₃NHCO(CH₂)₂OOCCHCH₂}]₂]^{4−}, while peaks observed at *m/z* 1038.58 and 1679.35 correspond to molecular fragments of {H[(SiW₁₁O₃₉)O{Si(CH₂)₃NHCO(CH₂)₂-OOCCHCH₂}]₂}]^{3−} and {(TBA)H[(SiW₁₁O₃₉)O{Si(CH₂)₃NHCO(CH₂)₂OOCCHCH₂}]₂}]^{2−}, respectively (See ESI for detailed information).

To get an insight into how the polymer network based on polymerizable POM nanoparticle (POM monomer) affects the BP behavior, we fabricated two samples with different monomer concentrations, where indiacrylate LC monomer C6M was used as a crosslinker and the compositions of these LC samples are listed in Table 2. As listed in Table 2, samples C1 and C2 contain the same POM monomer (1.0 wt%) but different C6M (0.5 wt% and 1.0 wt%). It is worth noting that the reason why the concentration of POM monomer we used is 1.0 wt% derives from the best doped concentration of unpolymerizable POM nanoparticle in BP system as mentioned above. In addition, the effective solubility of POM monomer in the bulk LCs is another factor to be considered. For the purpose of photo polymerization, the samples C1 and C2 were illuminated with a UV light (1.5 mW/cm², 365 nm) for 15 min, and the polymerization temperature was chosen as Ti-T = 3°C. After UV irradiation, the polymer network stabilized BP cell was examined again with polarized light microscope. By comparing the measured BP temperature range of the samples C1 and C2 with the case of no polymer network, we find that there is a little increase of the BP temperature range for both the samples before polymerization and after polymerization. In addition, BP temperature ranges for these three samples after polymerization have a further increase. As an example, for the sample C1 containing 1.0 wt% POM monomer and 0.5 wt% C6M, ΔT of BP is 8.9°C before polymerization. However, ΔT of BP after UV polymerization could reach to 16.3°C ranging from 51.5°C to 35.2°C, which means that the polymer network formed after UV polymerization have a positive effect on the BP stabilization. Figs. 5c and 5d show the polarized light microscope textures of the sample C1 in BP temperature range before and after polymerization, it could be observed that the BP structures were well kept after photo polymerization. In addition, it should be noted that increasing the C6M concentration does not further broaden the BP temperature range in sample C2 after polymerization. We think this may be due to that POM monomer with a branched structure of the side alkyl group may easily occupy into disclination lines. Meanwhile, due to the huge molecule volume of POM monomer, C6M as a crosslinker could just help POM monomers to undergo photo polymerization reaction, thereby leading to a formation of polymer network. Even if the concentration of C6M increases, the dominant role of POM monomer does not change. Therefore, increasing the concentration of C6M in the LC system does not have any significant effect on the BPs stabilization.

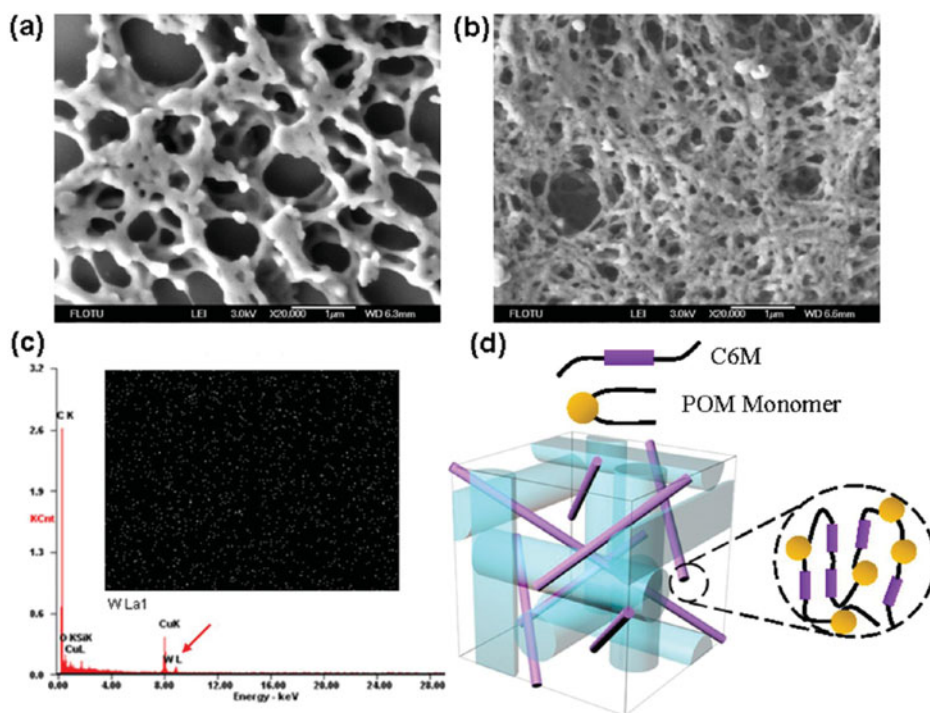


Figure 6. (a): SEM image of polymer network morphology of sample C1 after polymerization; (b): SEM image of polymer network morphology of sample C2 after polymerization; (c): EDX spectrum of the polymer network of sample C1; Inset image is EDX elemental map and (d): Schematic of polymer network structure within a cubic lattice of a polymer-stabilized BPs.

Fig. 6a and 6b exhibit scanning electron microscopy (SEM) images of the polymer network from the photo polymerization of POM nanoparticle and C6M in sample C1 and C2. Here the samples for investigating the polymer network were obtained by extracting non-reactive components from the LC cell with cyclohexane. It could be observed that the porous structures of polymer network are clearly visible in the SEM images. Additionally, it is obvious that the polymer network become intensive in sample C2 compared to that of sample C1 due to the increase of C6M concentrations. To confirm the formation of the polymer from the POM nanoparticles, the spatial distribution of metal elements in polymer network has been examined using energy-dispersive X-ray (EDX) elemental mapping analysis. As illustrated in Fig. 6c, EDX spectrum could tell us the existence of the tungsten (W), and the W element represented by white dots was homogeneously distributed in the polymer network as shown in the inset image of Fig. 6c. All these observations demonstrate that POM monomers participated in the formation of polymer network. Polymer-based stabilization of BP is well known and has been achieved previously in many LC systems, which is great effective to stabilize the BP. However, the demonstrated LC system here could further tell us what component comes into the disclination lines. That is to say, the POM moiety in this monomer as a marker could demonstrate what happens in the LC system during the photo polymerization.

Fig. 6d shows a simulated polymer network structure within a cubic lattice of a polymer stabilized BPs as mentioned in the previous study [13]. Here polymerizable POM nanoparticle just like unpolymerizable POM nanoparticle may be more miscible with an isotropic region than with a double-twist region due to their structure nature. Therefore, we think that the polymerizable POM nanoparticle may still stay at defect regions before UV irradiation

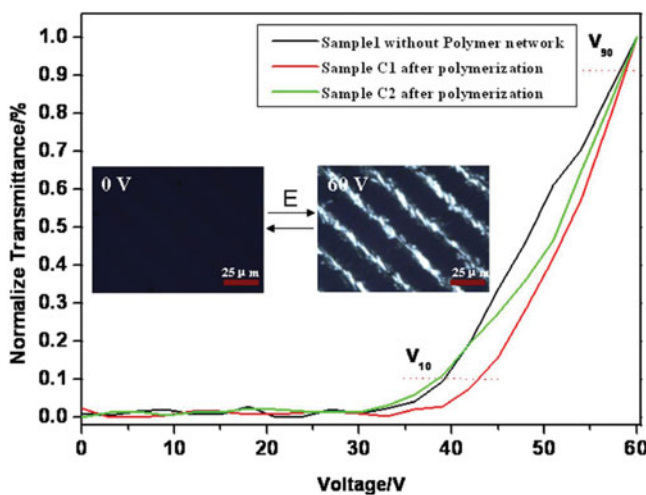


Figure 7. Normalized transmittance-voltage curves of samples A0 without polymer network (at 49°C), sample C1 (at 43°C) and sample C2 (at 42°C). The inset images of POM photos of the BPI of sample C2 after polymerization under the in-plane electric field geometry without the applied voltage and with the applied voltage of 60.0 V.

or move into the defect regions during UV irradiation. As a result, polymerization of the monomers forms a specific polymer networks with disclination array as shown in Fig. 6d. The right-hand side image in Fig. 6d could tell us that the organic-inorganic hybrid POM monomers are located at the joints of the polymer network. This may be due to the fact that POM monomers have a lower surface energy than that of C6M and may be easier to phase separates into the region of defects [35].

3.3. Electric-optical switching in polymer-stabilized BP based on Kerr effect

Electro-optical response of polymer stabilized BPs based on Kerr effect has been widely investigated due to the great potential in LCD fields [4]. To estimate the effect of polymer network on the electrical-optical performance, we measured the optical transmittance of the LC cells under crossed polarizers as a function of an applied electric field. Here the voltage for the increase in the transmittance from the initial state to 10% of the saturated state is defined as the threshold voltage, while the turn on voltage is the voltage for the increase in the transmittance from the initial state to 90% of the saturated state. As shown in Fig. 7, for the pure BP sample without polymer network, the threshold voltage is 39.17 V and the saturated voltage is 58.10 V. Meanwhile, the threshold voltages for the polymer stabilized samples C1 and C2 are 42.82 and 38.15 V, respectively. And the saturated voltages for these two samples are 58.64 and 58.36 V, respectively. These results demonstrate that both the threshold voltage and turn on voltage of the sample C1 increase a little when compared with the measured electro-optical switching characteristics of the control LC cell (without polymer network). However, the threshold voltage for the sample C2 is lower than that of the pure BP-LC sample, and the turn on voltage of these two samples are similar. Based on these observations, it is clear from the results that sample C2 shows the compatible electric-optical response due to the anchoring energy of polymer network formed by POM monomer and C6M. When compared sample C2 with sample C1, increasing the concentration of C6M (as a crosslinker) in LC mixture may lead to the enhancement of the polymerization efficiency of POM monomer, yielding a low

surface energy in BP-LC system. This is because that the polymerized POM monomers which disrupt any tendency toward orientational order inside the core of the BP and enable a weak anchoring at the surface of the inorganic nanoparticles. In addition, we note that these observations are different from that of the conventional polymer stabilized BP system, in which the threshold and turn on voltages greatly increase as the concentration of the polymer network is increased [24]. As shown the inset images in Fig. 7, a dark state for the sample C2 was obtained at the optically isotropic BPI state in the absence of the electric field, whereas a bright state could be observed when the applied voltage is 60.0 V. Furthermore, BPI could still reverse back to its original state after many switching circles, thus allowing us for the reversibly and dynamically switching of BPI. Based on these observations, the study demonstrated here provide a effective method to improve the electric-optical performances of the new promising BP display device.

4. Conclusions

To summarize, we have demonstrated a new kind of POM-based nanomaterials for the stabilization and electric-optical switching of BPs. First, the unpolymerizable POM-based nanoparticles (POM precursor and aggregates) were used to extend the temperature range of BPs. The results demonstrate that the temperature ranges of BPs could be significantly influenced by unpolymerizable POM-based nanoparticles, in which the widest BP temperature range could reach to 17.4°C. Second, the UV-polymerizable POM-based nanoparticle that could form polymer network after UV irradiation has been further developed. Polymerizable POM nanoparticle-based polymer networks, which were confirmed by SEM and EDX, were also found to have positive influence for stabilization of BPs. The stabilization mechanisms of both these two LC systems could attribute to a decrease in the free energy caused by self-organization-assisted nanoparticles assembly and POM-based polymer networks within disclination lines. Finally, the introduction of POM nanoparticle-based hybrid polymer network with a suitable concentration leads to a reduction in the switching voltage of the corresponding device, which we think is due to the low-surface energy characteristic of POM-based nanoparticle. These results provide a valuable insight into the organic-inorganic hybrid nanoparticle/polymer network for the stabilization of BP.

Acknowledgments

This research was supported by National Natural Science foundation (Grant No. 51373013 and 21222104), Beijing Young Talents Plan (YETP0489), the Fundamental Research Funds for the Central Universities (RC1302, YS1406) and Beijing Engineering Center for Hierarchical Catalysts.

References

- [1] Stamatiou, O., Mirzaei, J., Feng, X., & Hegmann, T. (2012). *Top Curr. Chem.*, 318, 331.
- [2] Bisoyi, H. K., & Kumar, S. (2011). *Chem. Soc. Rev.*, 40, 306.
- [3] Crooker, P. P., Kitzerow, H. S., & Bahr, C. (2001). *Chirality in liquid crystals[M]*, Springer: New York, 7, 186.
- [4] Kikuchi, H., Yokota, M., Hisakado, Y., Yang H., & Kajiyama, T. (2002). *Nat. Mater.*, 1, 64.
- [5] Cao, W., Munoz, A., Palffy-Muhoray, P., & Taheri, B. (2002). *Nat. Mater.*, 1, 111.
- [6] Coles, H.J., & Pivnenko, M. N. (2005). *Nature*, 436, 997.
- [7] Lavrentovich, O. D. (2011). *Proc. Natl. Acad. Sci.*, 108, 5143.

- [8] Lin, T. H., Li, Y., Wang, C. T., Jau, H. C., Chen, C. W., Li, C. C., Bisoyi, H. K., Bunning, T. J., & Li, Q. (2013). *Adv. Mater.*, 25, 5050.
- [9] Guo, J. B., Wang, J., Zhang, J. Y., Shi, Y., Wang, X. W., & Wei, J. (2014). *J. Mater. Chem. C.*, 2, 9159.
- [10] Jin, O. Y., Fu, D. W., Wei, J., Yang H., & Guo, J. B. (2014). *RSC Adv.*, 4, 28597.
- [11] Shi, Y., Mo, J., Wei, J., & Guo, J. B. (2015). *New J. Chem.*, 39, 1899.
- [12] Yoshizawa, A. (2013). *RSC Adv.*, 3, 25475.
- [13] Castles, F., Day, F. V., Morris, S. M., Ko, D. H., Gardiner, D. J., Qasim, M. M., Nosheen, S., Hands, P. J., Choi, S. S., Friend, R. H., & Coles, H. J. (2012). *Nat. Mater.*, 11, 599.
- [14] Wright, D. C., & Mermin, N. D. (1989). *Rev. Mod. Phys.*, 61, 385.
- [15] He, W. L., Pan, G. H., Yang, Z., Zhao, D. Y., Niu, G. G., Huang, W., Yuan, X. T., Guo, J. B., Cao, H., & Yang, H. (2009). *Adv. Mater.*, 21, 2050.
- [16] Henrich, O., Stratford, K., Cates, M. E., & Marenduzzo, D. (2011). *Phys. Rev. Lett.*, 106, 107801.
- [17] Dierking, I., Blenkhorn, W., Credland, E., Drake, W., Kociuruba, R., Kayser, B., & Michael, T. (2012). *Soft Matter*, 8, 4355.
- [18] Shibayama, S., Higuchi, H., Okumura Y., & Kikuchi, H. (2013). *Adv. Funct. Mater.*, 23, 2387.
- [19] Guo, J. B., Shi, Y., Han, X., Jin, O. Y., Wei, J., & Yang, H. (2013). *J. Mater. Chem. C.*, 1, 947.
- [20] Shi, Y., Wang, X. W., Wei, J., Yang, H., & Guo, J. B. (2013). *Soft Matter*, 9, 10186.
- [21] Wang, J., Lin, C. G., Zhang, J. Y., Wei, J., Song, Y. F., & Guo, J. B. (2015). *J. Mater. Chem. C.*, 3, 4179.
- [22] Xu, D. M., Yuan, J. M., Schadt M., & Wu, S. T. (2014). *Appl. Phys. Lett.*, 105, 081114.
- [23] Yoshida, H., Tanaka, Y., Kawamoto, K., Kubo, H., Tsuda, T., Fujii, A., Kuwabata, S., Kikuchi H., & Ozaki, M. (2009). *Appl. Phys. Express*, 2, 121501.
- [24] Karatairi, E., Rozic, B., Kutnjak, A., Tzitzios, V., Nounesis, G., Cordoyiannis, G., Thoen, J., Glo-rieux, C., & Kralj, S. (2010). *Phys. Rev. E.*, 81, 041703.
- [25] Wang, L., He, W. L., Xiao, X., Meng, F. G., Zhang, Y., Yang, P. Y., Wang, L. P., Xiao, J. M., Yang, H., & Lu, Y. F. (2012). *Small*, 8, 2189.
- [26] Ravnik, M., Alexander, G. P., Yeomans, J. M., & Žumer, S. (2011). *Proc. Natl. Acad. Sci.*, 108, 5188.
- [27] Song, Y. F., & Tsunashima, R. (2012). *Chem. Soc. Rev.*, 41, 7384.
- [28] Zheng, S. T., & Yang, G. Y. (2012). *Chem. Soc. Rev.*, 41, 7623.
- [29] Busche, C., Vilá-Nadal, L., Yan, J., Miras, H. N., Long, D. L., Georgiev, V. P., Asenoc, A., Pedersen, R. H., Gadegaard, N., Mirza, M.M., Paul, D. J., Poblet, J.M., & Cronin, L. (2014). *Nature*, 515, 545.
- [30] Cronin, L., & Müller, A. (2012). *Chem. Soc. Rev.*, 41, 7325.
- [31] Chen, W., Ma, D., Yan, J., Boyd, T., Cronin, L., Long, D. L., & Song, Y. F. (2013). *Chem Plus Chem.*, 78, 1226.
- [32] Lin, C. G., Chen, W., Omwoma, S., & Song, Y. F. (2015). *J. Mater. Chem. C.*, 3, 15.
- [33] Broer, D. J., Boven, J., Mol, G. N., & Challa, G. (1989). *Makromol. Chem.*, 190, 2255.
- [34] Bar-Nahum, I., Cohen, H., & Neumann, R. (2003). *Inorg. Chem.*, 42, 3677.
- [35] Kemiklioglu, E., Hwang, J. Y., & Chien, L. C. (2014). *Phy. Rev. E.*, 89, 042502.